PROCEEDINGS OF THE ROYAL SOCIETY B

Proc. R. Soc. B (2010) **277**, 337–344
doi:10.1098/rspb.2009.0149
Published online 29 April 2009

A new *Homo erectus* (Zhoukoudian V) brain endocast from China

Xiujie Wu[1,*], Lynne A. Schepartz[2] and Wu Liu[1]

[1]*Institute of Vertebrate Paleontology and Paleoanthropology, Chinese Academy of Sciences, Beijing 100044, People's Republic of China*
[2]*Department of Anthropology, Florida State University, Tallahassee, FL 32306-7772, USA*

A new *Homo erectus* endocast, Zhoukoudian (ZKD) V, is assessed by comparing it with ZKD II, ZKD III, ZKD X, ZKD XI, ZKD XII, Hexian, Trinil II, Sambungmacan (Sm) 3, Sangiran 2, Sangiran 17, KNM-ER 3733, KNM-WT 15 000, Kabwe, Liujiang and 31 modern Chinese. The endocast of ZKD V has an estimated endocranial volume of 1140 ml. As the geological age of ZKD V is younger than the other ZKD *H. erectus*, evolutionary changes in brain morphology are evaluated. The brain size of the ZKD specimens increases slightly over time. Compared with the other ZKD endocasts, ZKD V shows important differences, including broader frontal and occipital lobes, some indication of fuller parietal lobes, and relatively large brain size that reflect significant trends documented in later hominin brain evolution. Bivariate and principal component analyses indicate that geographical variation does not characterize the ZKD, African and other Asian specimens. The ZKD endocasts share some common morphological and morphometric features with other *H. erectus* endocasts that distinguish them from *Homo sapiens*.

Keywords: Zhoukoudian V; endocasts; *Homo erectus*; morphological and morphometric features; brain evolution

1. INTRODUCTION

The cranium of the Zhoukoudian (ZKD) V, *Homo erectus*, consists of four fragments found in two periods of excavation over a span of 32 years. The first fragment, found in June 1934 during excavation in layer three, Locus H III of ZKD locality 1, consisted of left temporal bone portions and adjoining parts of parietal and occipital. A second small fragment of the right temporal bone with the tympanic region was recognized when material from the same locus was prepared in the laboratory later that year (Weidenreich 1943). Another two fragments were found in 1966 (Qiu *et al.* 1973): the frontal squama with the brow and nasion region, along with parts of the sphenoid greater wing and parietal bone; and another fragment with the right half of the occipital and portions of parietal. When the discoveries of 1966 were compared with fragments from the same locus identified in 1934, it was determined that they belonged to the same individual, named ZKD V. Although the individual fragments exhibit slight post-mortem damage along their edges, they articulate to form a band of contiguous pieces with the largest gap (less than 5 mm) between the left frontal and temporal. The cranium and endocast (figure 1) were reconstructed in 1973. The endocast is rather complete, although it lacks portions of the parietal lobes and most of the base. The estimated volume is 1140 ml (Qiu *et al.* 1973).

ZKD V is of particular interest as it is geologically the youngest of the ZKD cranial series. An age of approximately 0.230 Ma was initially assigned based on U-series dating of mammalian fossils (Zhao *et al.* 1985). Electron spin resonance (ESR) dating of tooth enamel suggested that the geological age of ZKD V is 0.295–0.245 Ma (Huang *et al.* 1993). Subsequent ESR dating of mammalian teeth collected from layers three, 6/7 and 10 at locality 1, provided an age range of 0.300–0.550 Ma for the *H. erectus* sequence, with the age of ZKD V at *ca* 0.290 Ma (Grün *et al.* 1997). The ages of the locality 1 strata were remeasured by thermal ionization mass spectrometric U-series dating, and most recently using $^{26}Al/^{10}Be$ on buried quartz sediments and lithic artefacts from layers 7–10. The new results suggest that the age of ZKD V is more than 0.4 Ma, possibly in the range of approximately 0.4–0.5 Ma. ZKD III, from the lower stratum, is at least 0.6 ka and possibly more than 0.8 Ma (Shen *et al.* 2001, 2009) and thus much older than previously thought. The new age estimates imply that ZKD V was probably contemporaneous with the Hexian *H. erectus* that has an age of 0.412 Ma (Grün *et al.* 1998). While it is not currently possible to reconcile these two dating sequences for ZKD, it is important to emphasize that both document a clear range of ages for the ZKD stratigraphic sequence that is essential for understanding variation in the hominin sample.

Weidenreich (1935, 1943) studied the craniums of ZKD II, III, X, XI, XII and the portions of ZKD V that were then available. He suggested that the fundamental morphology of the ZKD crania remained unchanged over time. When Qiu *et al.* (1973) were able to study the more complete ZKD V cranium, they determined that it not only has the typical ZKD morphological characters, but also that it has what they described as more progressive features. For instance, the skull of ZKD V has a high and round temporal bone, a reduced occipital torus, and a

* Author for correspondence (wuxiujie@ivpp.ac.cn).

One contribution to a Special Issue 'Recent advances in Chinese palaeontology'.

Received 27 January 2009
Accepted 7 April 2009

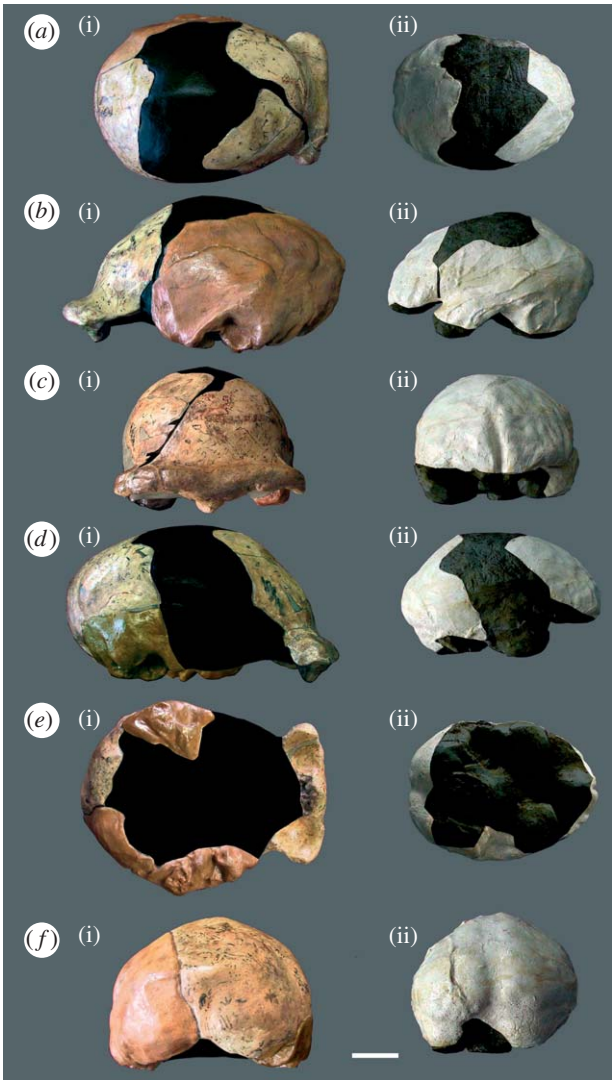

Figure 1. Reconstructed skull and endocast of ZKD V: (*a*(i)(ii)) superior view; (*b*(i)(ii)) left lateral view; (*c*(i)(ii)) anterior view; (*d*(i)(ii)) right lateral view; (*e*(i)(ii)) basal view; and (*f*(i)(ii)) posterior view. Reconstructed areas are shown in black. Scale bar, 4 cm.

short distance between inion and the internal occipital protuberance. Other evidence for temporal variation in ZKD *H. erectus* derives from studies of the human teeth (Zhang 1991) and the lithic industry (Pei & Zhang 1985).

In this paper, we analyse an unpublished endocranial cast of the ZKD V specimen and compare it with other *H. erectus* (ZKD II, III, X, XI, XII, Hexian, Sambungmacan (Sm) 3, Trinil II, Sangiran 2, Sangiran 17, KNM-ER 3733, KNM-WT 15 000) and *Homo sapiens* (Kabwe from Zambia, Liujiang from China, and a comparative modern Chinese sample). Our objective is to facilitate a more comprehensive understanding of ZKD *H. erectus* brain morphology and to re-examine the variability of *H. erectus*.

2. MATERIAL AND METHODS

(a) *Comparative samples*

Forty-six endocasts were included in the analysis as representative of China (ZKD V, III, II, X, XI, XII, Hexian, Liujiang and 31 modern Chinese), Indonesia (Sm 3, Trinil II, Sangiran 2, Sangiran 17) and Africa (KNM-ER 3733, KNM-WT 15 000 and Kabwe). Our fossil comparisons also represent the temporal span encompassing *H. erectus* through early *H. sapiens*. The geological ages of the sample specimens range from the earlier African specimens (KNM-ER 3733 at 1.75 Ma; Brown *et al.* 1985), KNM-WT 15 000 at 1.51 Ma (Brown & McDougall 1993) to the Indonesian group (Sm 3 and Trinil II at <1.0 Ma, Sangiran 2 dated to 0.7–1.6 Ma and Sangiran 17 at 0.7 Ma; Swisher *et al.* 1994; Delson *et al.* 2001), followed by Hexian (0.41 Ma; Grün *et al.* 1998), Kabwe (0.25 Ma; Vrba 1982) and Liujiang (0.067 Ma; Yuan *et al.* 1986). The observations and metric data for the Trinil II, Sm 3, Sangiran 2, Sangiran 17, KNM-ER 3733 and KNM-WT 15 000 endocasts are based on published data (Holloway 1981; Begun & Walker 1993; Broadfield *et al.* 2001; Holloway *et al.* 2004). The remaining data are from high quality endocasts in the collections of the Institute of Vertebrate Palaeontology and Paleoanthropology, Chinese Academy of Science.

(b) *Methods*

The research methodology employed here includes visual inspection and description of gross brain morphology and metrical analysis of size and shape differences. The landmarks and standardized measurements are detailed in Wu *et al.* (2006). During measurement, endocasts were placed on a flat surface with the horizontal plane along the axis of the frontal and occipital poles (right side) parallel to the flat surface. The specimen remained with the axis of the frontal and occipital poles parallel to the flat surface whether rotated for a superior or lateral view. Linear measurements included: the length (the greater of the two hemisphere lengths from the frontal pole to occipital pole); breadth (maximum width perpendicular to the sagittal plane); height (a projection from the highest point of the parietal lobe to the most ventral point of the cerebellar hemisphere); frontal breadth (maximum width of the frontal lobe); cerebral height (the highest point of the parietal lobe to the most ventral point of the temporal lobe); frontal height (a projection from bregma to the most ventral point of the frontal lobe); frontal chord (bregma to the frontal pole); parietal chord (bregma to lambda); and occipital breadth (maximum width of the occipital lobe perpendicular to the sagittal plane). Lengths, heights, cerebral heights, frontal heights and frontal chords were measured on the right side. Petalias were scored by comparing widths rather than rostral/caudal projections, following Zilles *et al.* (1996). The widths of the frontal lobes were measured at 20 per cent of the distance from their most anterior points and the widths of the occipital lobes were assessed at 10 per cent of the distance from their most posterior projection.

Statistical analyses were performed using SPSS (v. 11.0). Bivariate plots and principal component analyses (PCA) were used to examine the interactions among variables. In bivariate plot comparisons, length–breadth, length–height, breadth–frontal breadth and breadth–occipital breadth were used, and linear regression analysis with 95% confidence intervals was used to show the range of the modern Chinese. PCA requires that the ratio of cases to variables should be at least five to one. We ran two analyses that met or exceeded these parameters; one with 46 specimens and nine linear measures, and another with 46 specimens and six linear measures. For the second analysis, we excluded the two variables that have large values for the first component, and excluded one variable that has a large value for the second component based on the factor loading of the first analysis.

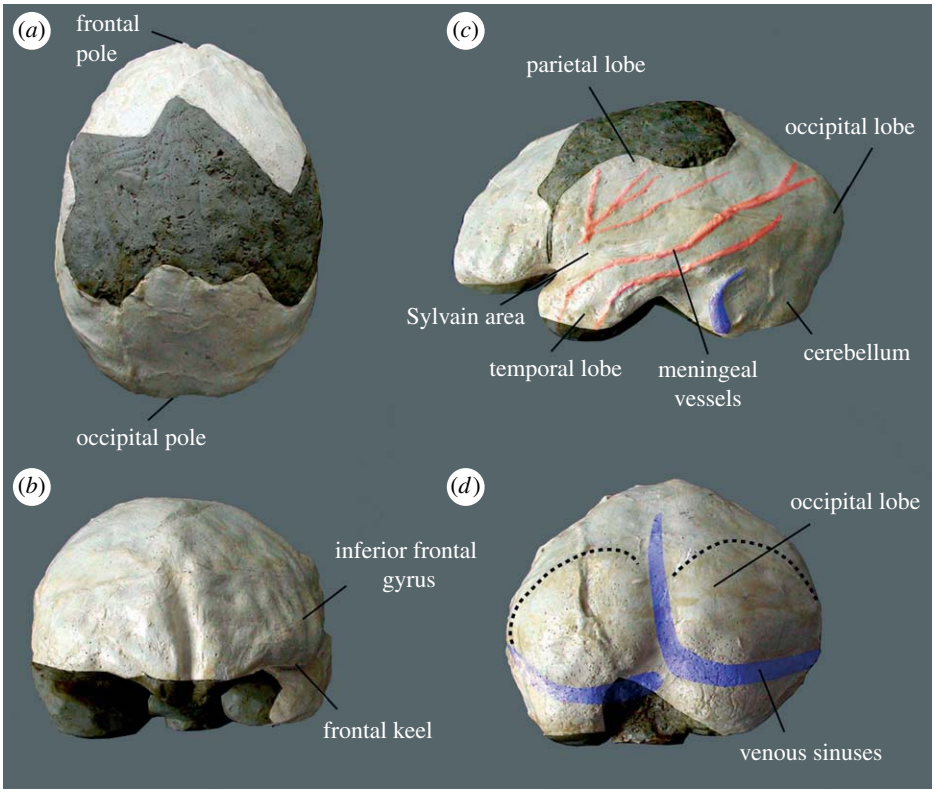

Figure 2. Morphological features of the ZKD V endocast. Views: (*a*) superior; (*b*) anterior; (*c*) left lateral; (*d*) posterior with limits of the occipital lobes denoted by dashed lines. Reconstructed areas shown in black.

3. RESULTS

(a) *Gross morphology of ZKD V*

The ZKD V endocast is long and narrow with an ovoid form in superior view (figure 2*a*). The widest point of ZKD V is situated at the lateral border of the temporal lobes. The frontal region is flattened bilaterally, when compared with modern humans, and bulges in the centre of the frontal lobe, while the orbital margin is full and culminates in a well-marked and prominent frontal keel. The area of the inferior frontal gyrus is slightly larger and more prominent on the left side (figure 2*b*). According to the small preserved part on the left displaying the meningeal vessels (figure 2*c*), the parietal lobe appears to be filled-out rather than depressed. This differs from the clearly depressed areas seen on the other ZKD specimens (Wu *et al*. 2006). As the top of the parietal lobes is missing, it is not possible to determine if ZKD V has the sagittal keel that is observed on the other ZKD endocasts.

The temporal lobes of ZKD V are narrow and bulging, and the Sylvain area between the temporal and frontal lobes shows a distinct depression (figure 2*c*). The occipital poles are especially prominent and rounded, and have strong posterior projection (figure 2*c*). The superior portion of the occipital lobe forms a semicircular shape (figure 2*d*). The middle meningeal vessels appear clearly on the left side. They divide into a short anterior branch that courses towards the frontal parietal pole and two parallel longer posterior branches that course caudally and become elaborated in the region of the occipital parietal cortex (figure 2*b*). The superior sagittal sinus is visible above lambda at the vertex of the division between the occipital lobes. Inferiorly, the vessel deviates somewhat to the right and is continuous with the right transverse sinus at the confluence, sweeping forward and downward to the right sigmoid sinus and then into the right jugular region (figure 2*d*).

Based upon our comparisons of the relative widths of the frontal and occipital lobes, ZKD V manifests a right frontal and left occipital petalia pattern.

(b) *Morphological comparison*

In superior view, the shapes of the endocasts in our study are all basically elliptical although some endocasts, such as ZKD III, Trinil II and KNM-WT 15 000, have relatively narrow frontal lobes and broader parietal lobes. The widest point of ZKD V is low on the parietal lobes (a feature shared with all the *H. erectus* in our sample), while the widest point of Kabwe, Liujiang and the modern Chinese endocasts is high and situated at approximately the midpoint of the total brain height. The surfaces of the frontal lobe of ZKD V, the other ZKD endocasts, Hexian, Trinil II, Sangiran 2, Sangiran 17, KNM-ER 3733 and KNM-WT 15 000 are all flat, whereas the frontal lobes of Sm 3, Kabwe, Liujiang and the modern Chinese are full and rounded. ZKD V, III, XI, XII, Hexian, Trinil II and Sangiran 17 have a well-marked and prominent frontal keel that is not seen on Sm 3, KNM-ER 3733, KNM-WT 15 000, Kabwe or Liujiang. The orbital margin is rounded and no prominent frontal keel is seen in any of the modern Chinese. All of the endocasts examined here also have slight predominance of the left inferior frontal gyrus. The ZKD, Hexian (left side), Sangiran 17 and Kabwe endocasts have depressed Sylvian areas, in contrast to the undepressed regions that characterize Sm 3, Trinil II, Sangiran 2, KNM-ER 3733, KNM-WT 15 000 and the modern Chinese.

Superiorly, the parietal lobes of ZKD II, III, X, XI, XII, Kabwe and Hexian are depressed and slope downward in all directions from the centro-vertex (the most superior point on the midline separating the parietal lobes); in KNM-WT 15 000, Sm 3, Trinil II, Sangiran 2, Sangiran 17, Liujiang and the modern Chinese the parietal lobe is round and full. The small portion of the parietal lobe preserved on the ZKD V endocasts also appears to be round and full. The temporal lobes of the ZKD endocasts and Kabwe are narrow and slender. By contrast, Hexian, Sm 3, Trinil II, Sangiran 2, Sangiran 17, KNM-ER 3733, KNM-WT 15 000 and the modern Chinese have fuller and broader temporal lobes. The occipital lobes of the ZKD endocasts, Hexian, Sangiran 2, Sangiran 17, Kabwe and Liujiang are dorsoventrally flattened and have strong posterior projections. Sm 3, Trinil II, KNM-ER 3733, KNM-WT 15 000 and the modern Chinese have round occipital lobes that lack strong posterior projections. The cerebellum of ZKD V is low and located under the occipital poles, and the cerebellar structures are quite separated. This form is seen in all the fossil hominin endocasts in our sample, but it differs from that of the modern Chinese where the cerebellar structures are more globular and approach the midline.

The meningeal vessels of ZKD V are similar to the other ZKD *H. erectus*, Hexian, Sangiran 17, Sangiran 2, Trinil II, and Sm 3 in that more branches overlie the middle to posterior regions. The anterior branch of the middle meningeal system appears to be more developed on KNM-WT 15 000 (Begun & Walker 1993) and Kabwe (Holloway *et al.* 2004). In modern Chinese, the anterior and middle rami of the middle meningeal vessels are very developed and send more branches to the parietal–temporal region, while the posterior ramus sends limited branches to the occipital region.

The form of the venous sinuses varies among the endocasts we examined and there are no distinct patterns that distinguish any group of specimens.

ZKD V manifests an R-frontal and L-occipital petalia width pattern, which is the pattern characteristic of most modern humans (cf. Holloway & De La Coste-Lareyondie 1982; Zilles *et al.* 1996). ZKD III has a R-frontal and R-occipital petalial width pattern, while ZKD X has L-frontal and R-occipital and ZKD XI and XII have L-frontal and L-occipital patterns.

(c) *Bivariate morphometric analysis*

Nine standardized measurements were taken on ZKD V and the comparative endocasts (table 1). Bivariate plots of selected measures (figure 3) illustrate general size trends in the sample. The results of a linear regression with a 95% individual prediction interval for the modern Chinese sample are plotted for comparison.

Figure 3*a* is a plot of length and breadth. ZKD V is most similar to ZKD X in length and breadth. ZKD V, II, X, XI, XII, KNM-WT 15 000, Kabwe and Liujiang are within the 95% confidence interval for the modern Chinese. By contrast, Sangiran 17, Sangiran 2, Hexian, ZKD III, Trinil II, Sm 3, and KNM-ER 3733 fall below the 95% confidence limit.

Figure 3*b* is a plot of length and height. ZKD V is quite long relative to its height, and lies close to ZKD X, XI, XII and Kabwe. All the fossil endocasts, with the

Table 1. Endocast measurements (mm).

specimens	length	breadth	height	frontal breadth	cerebral height	frontal height	frontal chord	parietal chord	occipital breadth	cranial capacity
ZKD V	174.9	128.0	108.2	110.1	108.9	74.8	82.0	87.1	99.1	1140; Qiu *et al.* (1973)
ZKD III	156.1	120.4	99.7	91.9	98.9	73.1	78.2	86.9	87.3	915; Weidenreich (1943)
ZKD II	161.1	116.2	106.4	94.2	107.2	78.2	75.9	94.5	89.9	1020; Weidenreich (1943)
ZKD X	174.2	128.7	114.8	106.7	116.2	88.2	85.3	95.9	95.5	1225; Weidenreich (1943)
ZKD XI	166.1	127.2	103.7	97.1	105.4	79.0	70.2	87.2	93.3	1015; Weidenreich (1943)
ZKD XII	167.6	127.8	108.5	97.8	107.3	79.9	82.6	87.5	95.0	1030; Weidenreich (1943)
Hexian	159.4	134.8	100.7	99.8	102.0	75.9	69.1	92.2	96.6	1025; Wu & Dong (1982)
Liujiang	175.5	136.1	125.3	115.2	112.2	94.5	89.1	107.1	101.9	1567; Wu *et al.* (2008)
Sambungmacan 3	151.1	113.6	107.2	103.5	101.3	75.0	73.0	82.9	95.6	917; Broadfield *et al.* (2001)
Trinil II	156.1	125.4	97.9	94.3	102.1	77.9	75.6	83.0	92.2	940; Holloway (1981)
Sangiran 2	148.0	120.0	89.8	93.7	93.0	70.3	68.4	70.0	92.0	813; Holloway (1981)
Sangiran 17	161.0	131.0	97.5	108.5	97.0	72.0	73.9	93.0	101.0	1004; Holloway (1981)
KNM-ER 3733	146.0	122.0	98.5	102.2	97.0	73.1	71.9	97.0	95.0	848; Holloway (1981)
KNM-WT 15 000	158.0	116.0	100.0	86.0	107.0	66.0	73.0	93.0	103.0	880; Begun & Walker (1993)
Kabwe	173.5	138.5	115.5	108.0	117.9	88.0	77.6	103.9	110.9	1280; Rightmire (2004)
Modern Chinese ($n = 31$)	159.8–177.0	117.0–137.3	119.8–135.2	102.9–122.3	110.9–133.8	86.1–99.9	69.2–89.0	97.9–114.1	91.5–107.5	1110–1600

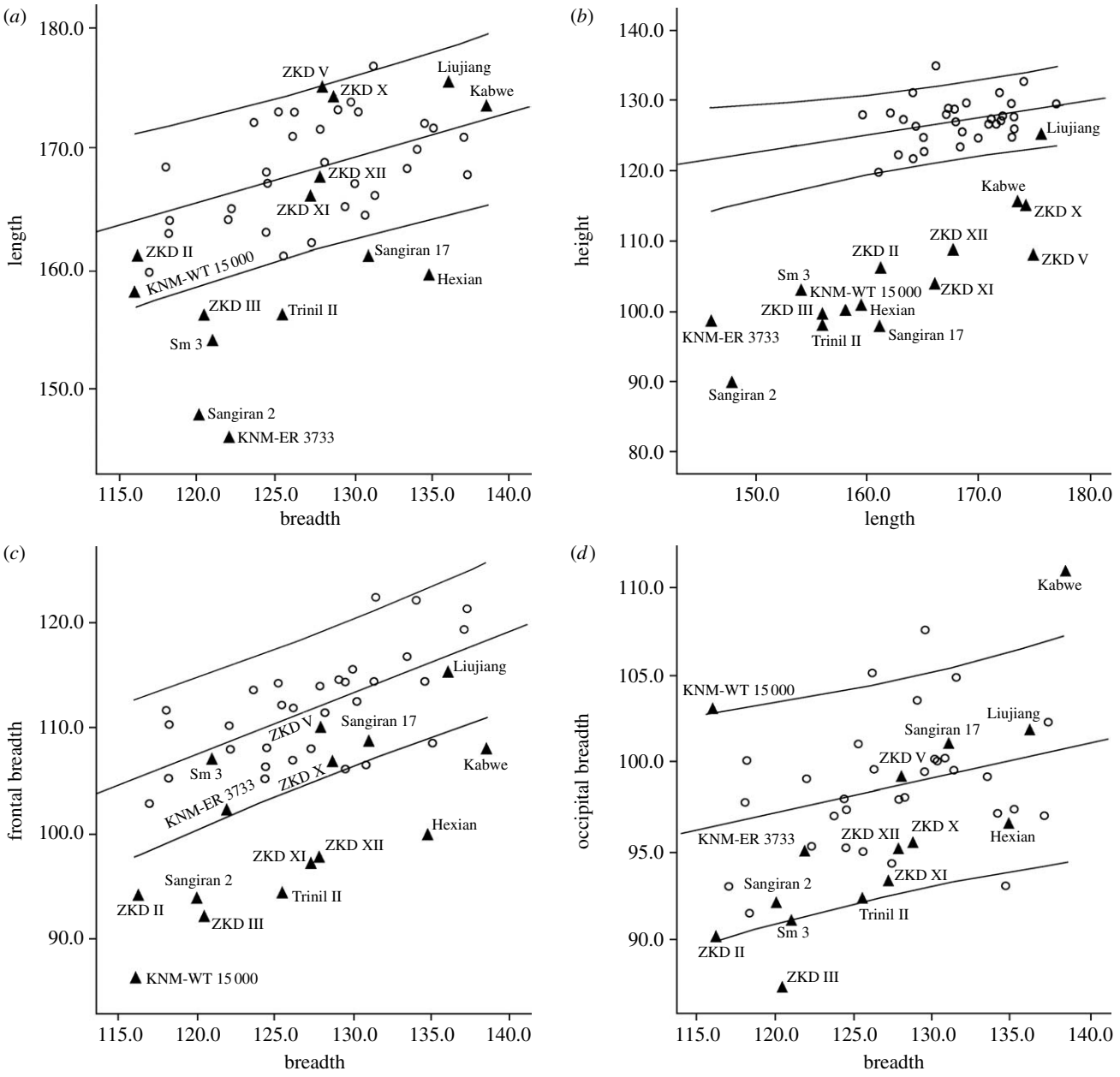

Figure 3. Bivariate plots of ZKD V and comparative endocasts: (*a*) breadth versus length; (*b*) length versus height; (*c*) breadth versus frontal breadth; (*d*) breadth versus occipital breadth. Linear regression with 95% individual prediction interval is presented for the modern Chinese specimens represented by circles.

exception of Liujiang, are below the 95% confidence interval for the modern Chinese.

In the plot of breadth and frontal breadth (figure 3*c*), the frontal breadth of ZKD V is closest to ZKD X and Sangiran 17. ZKD V, X, Sangiran 17, Sm 3, KNM-ER 3733 and Liujiang are within the 95% interval for the modern Chinese endocasts while the frontal lobes of ZKD II, III, XI, XII, Hexian, Trinil II, Sangiran 2 and KNM-WT 15 000 are narrower than the modern Chinese.

Finally, in the comparison of breadth and occipital breadth (figure 3*d*), the occipital breadth of ZKD V is closest to Sangiran 17. All fossils except ZKD III, KNM-WT 15 000 and Kabwe are within the range of the modern Chinese predictive interval. The occipital lobes of ZKD III and ZKD II are narrower than the other fossils and the modern Chinese, while the occipital lobes of KNM-WT 15 000 and Kabwe are wider than the other endocasts.

(d) *Principal component analyses*

PCA provide further information on overall shape. In the nine-variable analysis (table 2), the first two components account for 74.3 per cent of the total variance. The first component (62.1%) has positive loadings on all variables, and is mainly related to the height and frontal height. The second component (12.2%) is mainly related to the breadth and occipital breadth. In figure 4*a*, ZKD V is closer to Sangiran 17, Hexian and ZKD 12 and distant from Sangiran 2, ZKD II and ZKD III. ZKD X and Liujiang are in the range of the modern Chinese.

In the six-variable analysis (table 2), we use the length, frontal breadth, cerebral height, frontal chord, parietal chord and occipital chord. The excluded variables are breadth, height and frontal height, which have high scores based on the factor loading of the nine-variable analysis. The first and second principal components represent

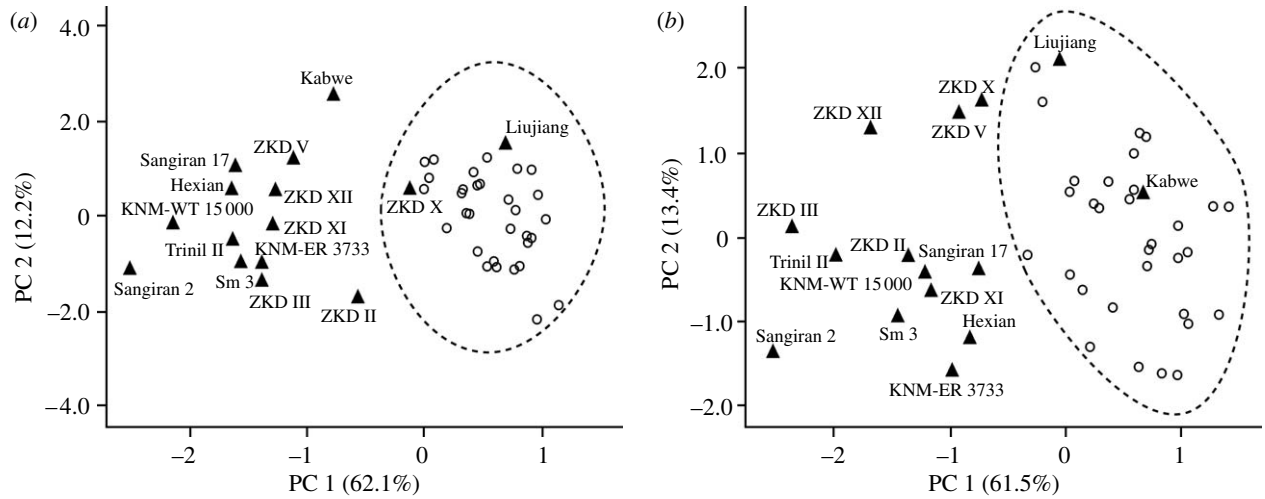

Figure 4. PCA of ZKD V, other fossils and modern Chinese endocasts (circles enclosed by the dashed line). (*a*) Nine-variable PCA; and (*b*) six-variable PCA.

Table 2. Principal components analysis loadings: nine-variable and six-variable analyses of ZKD V, other *H. erectus*, Kabwe, Liujiang and modern Chinese endocasts.

	nine-variable		six-variable	
variable	PC 1	PC 2	PC 1	PC 2
length	0.829	0.253	0.864	0.258
breadth	0.557	0.659		
height	0.917	−0.337		
frontal breadth	0.824	0.041	0.806	−0.251
cerebral height	0.887	−0.312	0.855	−282
frontal height	0.910	−0.243		
frontal chord	0.580	0.199	0.627	0.724
parietal chord	0.882	−0.229	0.876	−0.265
occipital chord	0.584	0.484	0.636	−0.01
percentage of variance	62.1	12.2	61.5	13.4

61.5 and 13.4 per cent of the total variance. The first component is related to the length and the parietal chord, and the second component is related to the frontal chord. In figure 4*b*, ZKD V is closest to ZKD X and ZKD XII. ZKD III, II, Hexian, Sm 3, Trinil II, Sangiran 2, Sangiran 17, KNM-ER 3733 and KNM-WT 15 000 cluster together. Liujiang and Kabwe are in the range of the modern Chinese.

4. DISCUSSION

The endocast of ZKD V has a volume of approximately 1140 ml (Qiu *et al.* 1973), which is in the upper range of endocranial volumes obtained for other *H. erectus* specimens (600–1251 ml; Rightmire 2004; Lee 2005), and in the lower end of the modern Chinese range in our sample (1110–1600 ml; table 1). At 1225 ml, ZKD X is the largest in the ZKD group (Weidenreich 1943), while the smallest modern Chinese endocast is only 1110 ml. These measures would seem to indicate that the volume of ZKD V is not very different from either the other *H. erectus* specimens or modern humans. The length, breadth, frontal breadth, frontal chord and occipital breadth for ZKD V are in the range of the modern Chinese (table 1). Height, cerebral height, frontal height and the parietal chord for ZKD V are smaller than the modern Chinese, and in the range of the *H. erectus* in our sample. The bivariate plots of length–breadth, length–height, breadth–frontal breadth and breadth–occipital breadth clearly indicate that height changed the most, but breadth did not change, in human brain evolution. For ZKD V, and to a lesser extent the sample from ZKD, the overall length is long compared with the other *H. erectus* in our sample. ZKD V also has bigger frontal and occipital lobes than the other ZKD specimens. The morphological features of ZKD V that are shared with other ZKD endocasts include the following: flattening of the frontal region; the appearance of the frontal cap as a salient landmark; temporal lobes that are narrow and bulging; occipital lobes that are dorsoventrally flattened and have strong posterior projection; low height of the cerebellar area and anterior positioning relative to the occipital lobe; and posterior branches of the middle meningeal arteries that are bigger than the anterior branches. The parietal lobes of ZKD V appear filled-out and bossed on both sides, which contrasts with the depressed, flatter parietal lobes of the other ZKD specimens.

The taxonomic affinity of the ZKD hominins has long been questioned. Previous analyses, mostly based on study of external cranial morphology, led researchers to propose that the ZKD crania possess unique morphological and morphometric features distinguishing them from other Asian as well as African hominins (Kidder 1998; Anton 2002, 2003; Kidder & Durband 2004). According to Anton (2002), regional differentiation exists between

northern Asian and southeast Asian *H. erectus*, and the ZKD *H. erectus* sample exhibits less variation than the early Indonesian sample. Other researchers argue that the cranial features thought to define Asian *H. erectus* are also expressed on some African specimens (Rightmire 1998). Differences between the Far Eastern and African hominins are viewed as minor and not indicative of more than one species (Braüer 1994).

Detailed endocast studies comparing Asian and other *H. erectus* specimens are limited in number. Begun & Walker (1993) suggested that the ZKD *H. erectus* endocasts are overall morphologically similar to KNM-WT 15 000. In a previous study, we found that Hexian from central-eastern China is morphologically most similar to the ZKD specimens (Wu *et al.* 2006). Interestingly, the nine-variable and six-variable PCA results of this study show that the six ZKD endocasts do not cluster together, and do not present a different pattern from the African or the other Asian specimens. Our research on endocast size and shape provides no support for the argument that ZKD *H. erectus* or other Asian *H. erectus* specimens represent a morphologically distinct species.

The ZKD sample has low brain height, a low position of the greatest breadth, flat frontal lobes, and a low and anterior positioning of the cerebellar lobes relative to the occipital lobes. These features are shown on the other *H. erectus* endocasts (Hexian, Trinil II, Sm 3, Sangiran 2, Sangiran 17, KNM-ER 3733 and KNM-WT 15 000) in our sample. The full orbital margin and prominent frontal keel of the ZKD endocasts can also be observed on Hexian, Trinil II and Sangiran 17. The form of the middle meningeal vessels is the one feature that appears to have undergone the greatest alteration during hominin evolution (cf. Falk (1993) and related discussion in Holloway *et al.* (2004) and Wu *et al.* (2006)). In our study, the relative simplicity of the meningeal patterns on the ZKD endocasts are similar to those of Hexian, Sangiran 17, Sangiran 2, Trinil II and Sm 3, while on KNM-WT 15 000 and *H. sapiens*, the anterior and middle rami are very developed and send more branches to the parietal–temporal region.

Our studies indicate that the ZKD endocasts share some morphological and morphometric features with the African and other Asian specimens that distinguish them from the modern Chinese comparative sample. We also note that the ZKD V endocast shows some progressive features compared with the other ZKD *H. erectus*—'progressive' in the sense that ZKD V differs in ways that foreshadow the greater overall brain height and fuller lobes that generally characterize *H. sapiens*. This is not unexpected given its later geological age and the possibility that as much as half a million years may be represented by the ZKD sample.

We are grateful to Yinyun Zhang for his help in preparing the endocast of ZKD V and the many important insights on human evolutionary processes that he has shared with us over the years. We also thank the reviewers for their helpful suggestions. This project is supported by the Knowledge Innovation Program of the Chinese Academy of Sciences (grant no. KZCX2-YW-106), Major Basic Research Projects (grant no. 2006CB806400), and the International Cooperation Program of MST of China (grant no. 2007DFB20330). W.X. gratefully acknowledges the support of the Chinese Academy of Sciences and K. C. Wong Education Foundation of Hong Kong.

REFERENCES

Anton, S. 2002 Evolutionary significance of cranial variation in Asian *Homo erectus*. *Am. J. Phys. Anthropol.* **118**, 301–323. (doi:10.1002/ajpa.10091)

Anton, S. 2003 Natural history of *Homo erectus*. *Yearb. Phys. Anthropol.* **46**, 126–170. (doi:10.1002/ajpa.10399)

Begun, D. & Walker, A. 1993 The endocast. In *The Nariokotome Homo erectus* skeleton (eds A. Walker & R. Leakey), pp. 326–358. Cambridge, MA: Harvard University Press.

Braüer, G. 1994 How different are Asian and African *Homo erectus*? *Cour. Forsch. Inst. Senckenberg* **171**, 301–318.

Broadfield, D. C., Holloway, R. L., Mowbray, K., Mowbray, K., Silvers, A., Yuan, M. S. & Márquez, S. 2001 Endocast of Sambungmacan 3 (Sm 3): a new *Homo erectus* from Indonesia. *Anat. Rec.* **262**, 369–379. (doi:10.1002/ar.1047)

Brown, F. H. & McDougall, I. 1993 Geologic setting and age. In *The Nariokotome Homo erectus* skeleton (eds A. Walker & R. Leakey), pp. 9–20. Cambridge, MA: Harvard University Press.

Brown, F. H., Harris, J., Leakey, R. & Walker, A. 1985 Early *Homo erectus* skeleton from west Lake Turkana, Kenya. *Nature* **316**, 788–792. (doi:10.1038/316788a0)

Delson, E., Harvati, K., Reddy, D., Marcus, L. F., Mowbray, K., Sawyer, G. J., Jacob, T. & Márquez, S. 2001 The Sambungmacan 3 *Homo erectus* calvaria: a comparative morphometric and morphological analysis. *Anat. Rec.* **262**, 380–397. (doi:10.1002/ar.1048)

Falk, D. 1993 Meningeal arterial patterns in great apes: implications for hominid vascular evolution. *Am. J. Phys. Anthropol.* **92**, 81–97. (doi:10.1002/ajpa.1330920107)

Grün, R., Huang, P. H., Wu, X. Z., Stringer, C. B., Thorne, A. G. & McCulloch, M. 1997 ESR analysis of teeth from the palaeoanthropological site of Zhoukoudian, China. *J. Hum. Evol.* **32**, 83–91. (doi:10.1006/jhev.1996.0094)

Grün, R., Huang, P. H., Huang, W. P., McDermott, F., Thorne, A., Stringer, C. B. & Yan, G. 1998 ESR and U-series analyses of teeth from the palaeoanthropological site of Hexian, Anhui Province, China. *J. Hum. Evol.* **34**, 555–564. (doi:10.1006/jhev.1997.0211)

Holloway, R. L. 1981 The Indonesian *Homo erectus* brain endocasts revisited. *Am. J. Phys. Anthropol.* **55**, 503–521. (doi:10.1002/ajpa.1330550412)

Holloway, R. L. & De La Coste-Lareyondie, M. C. 1982 Brain endocast asymmetry in pongids and hominids: some preliminary findings on the paleontology of cerebral dominance. *Am. J. Phys. Anthropol.* **58**, 101–110. (doi:10.1002/ajpa.1330580111)

Holloway, R. L., Broadfield, D. C. & Yuan, M. S. 2004 The human fossil record. *Brain endocasts—the paleoneurological evidence*, vol. 3. Hoboken, NJ: Wiley-Liss.

Huang, P. H. *et al.* 1993 ESR dating of tooth enamel: comparison with U-Series, FT and TL dating at the Peking Man Site. *Appl. Radia. Isotopes.* **44**, 239–242. (doi:10.1016/0969-8043(93)90226-Z)

Kidder, J. H. 1998 Morphometric variability in *Homo erectus*. *Am. J. Phys. Anthropol.* **24**(Suppl.), 138.

Kidder, J. H. & Durband, A. C. 2004 A re-evaluation of the metric diversity within *Homo erectus*. *J. Hum. Evol.* **46**, 297–313. (doi:10.1016/j.jhevol.2003.12.003)

Lee, S.-H. 2005 Brief communication: is variation in the cranial capacity of the Dmanisi sample too high to be from a single species? *Am. J. Phys. Anthropol.* **127**, 263–266. (doi:10.1002/ajpa.20105)

Pei, W. Z. & Zhang, S. S. 1985 A study on the lithic artifacts of *Sinanthropus*. *Palaeontol. Sin. New Ser. D* **12**, 1–277.

Qiu, Z. L., Gu, Y. M., Zhang, Y. Y. & Zhang, S. S. 1973 Newly discovered *Sinanthropus* remains and stone artifacts at Zhoukoudian. *Vertebr. PalAsiatica* **11**, 109–131.

Rightmire, G. P. 1998 Evidence from facial morphology for similarity of Asian and African representatives of *Homo erectus*. *Am. J. Phys. Anthropol.* **106**, 61–85. (doi:10.1002/(SICI)1096-8644(199805)106:1<61::AID-AJPA5>3.0.CO;2-G)

Rightmire, G. P. 2004 Brain size and encephalization in Early to Mid-Pleistocene *Homo*. *Am. J. Phys. Anthropol.* **124**, 109–123. (doi:10.1002/ajpa.10346)

Shen, G., Ku, T., Cheng, H., Edwards, R., Yuan, Z. & Wang, Q. 2001 High-precision U-series dating of locality 1 at Zhoukoudian, China. *J. Hum. Evol.* **41**, 679–688. (doi:10.1006/jhev.2001.0516)

Shen, G., Gao, X., Gao, B. & Granger, D. 2009 Age of Zhoukoudian *Homo erectus* determined with $^{26}Al/^{10}Be$ burial dating. *Nature* **458**, 198–200. (doi:10.1038/nature07741)

Swisher III, C. C., Curtis, G. H., Jacob, J., Getty, A. G., Suprijo, A. & Widiasmoro 1994 Age of the earliest known hominids in Java, Indonesia. *Science* **263**, 1118–1121. (doi:10.1126/science.8108729)

Vrba, E. S. 1982 Biostratigraphy and chronology, based particularly on Bovidae, of southern hominid-associated assemblages: Makapansgat, Sterkfontein, Taung, Kromdraai, Swartkrans; also Elandsfontein (Saldanha) Broken Hill (now Kabwe) and Cave of Hearths. In *L'Homo erectus et la place de l'homme de Tautavel permi les hominids fossils* (ed. M. A. de Lumley), pp. 707–752. Nice, France: Premier Congrès International de Paléontologie Humaine.

Weidenreich, F. 1935 The *Sinanthropus* population of Choukoutien (locality 1) with a preliminary report on new discoveries. *Bull. Geol. Soc. China* **14**, 427–461.

Weidenreich, F. 1943 The skull of *Sinanthropus pekinensis*: a comparative study on a primitive hominid skull. *Palaeontol. Sin. New Ser.* **10**, 108–113.

Wu, R. K. & Dong, X. R. 1982 Preliminary study of *Homo erectus* remains from Hexian, Anhui. *Acta Anthropol. Sin.* **1**, 2–13. [In Chinese.]

Wu, X. J., Schepartz, L. A., Falk, D. & Liu, W. 2006 Endocast of Hexian *Homo erectus* from south China. *Am. J. Phys. Anthropol.* **130**, 445–454. (doi:10.1002/ajpa.20378)

Wu, X. J., Liu, W., Dong, W., Qu, J. M. & Wang, Y. F. 2008 The brain morphology of *Homo* Liujiang cranium fossil by three-dimensional computed tomography. *Chin. Sci. Bull.* **53**, 2513–2519. (doi:10.1007/s11434-008-0263-z)

Yuan, S. X., Chen, T. M. & Gao, S. J. 1986 Uranium series chronological sequence of some Paleolithic sites in south China. *Acta Anthropol. Sin.* **5**, 179–190. [In Chinese.]

Zhang, Y. Y. 1991 An examination of temporal variation in the hominid dental sample from Zhoukoudian locality 1. *Acta Anthropol. Sin.* **10**, 85–95. [In Chinese.]

Zhao, S. S., Pei, J. X., Guo, S. L., Liu, S. S., Qian, F., Chou, S. H. & Li, X. G. 1985 Study of chronology of Peking Man site. In *Multi-disciplinary study of the Peking Man site at Zhoukoudian* (eds R. K. Wu, M. E. Ren, X. M. Zhu, Z. G. Yang, C. K. Hu, Z. C. Kong, Y. Y. Xie & S. S. Zhao), pp. 239–240. Beijing, China: Science Press.

Zilles, K., Dabringhaus, A., Geyer, S., Amunts, K., Qü, M., Schleicher, A., Gilissen, E., Schlaug, G. & Steinmetz, H. 1996 Structural asymmetries in the human forebrain and the forebrain of non-human primates and rats. *Neurosci. Biobehav. Rev.* **20**, 593–605. (doi:10.1016/0149-7634(95)00072-0)